CHAPTER 5

Automated robust proton planning using dose-volume histogram based mimicking of the photon reference dose and reducing organ at risk dose optimization

Kierkels, Roel G J
Fredriksson, Albin
Both, Stefan
Langendijk, Johannes A
Scandurra, Daniel
Korevaar, Erik W

Int. J. Radiat. Oncol. (2019) Volume 103, Issue 1, Pages 251 - 258

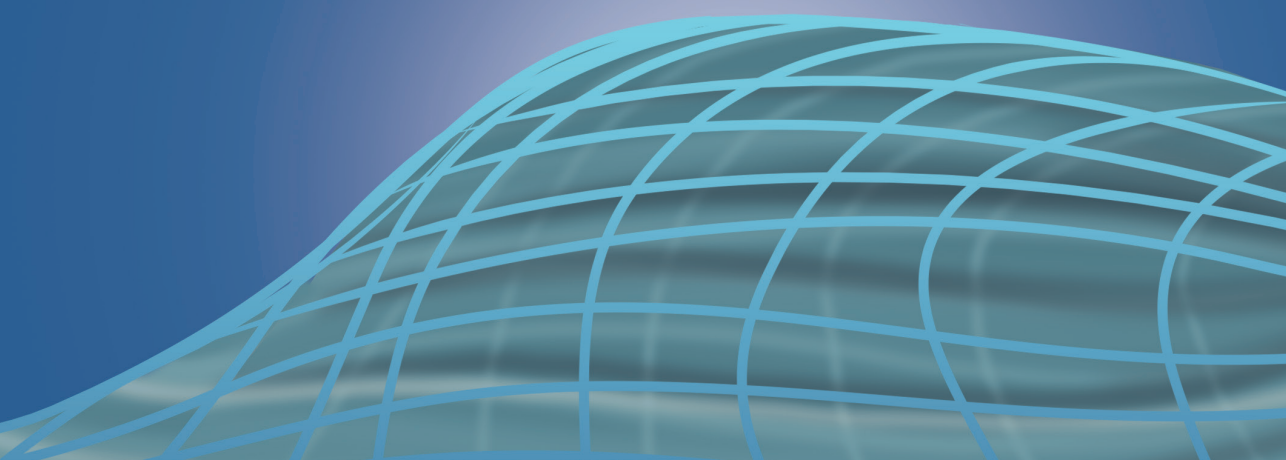

Abstract

Patient selection for proton therapy is increasingly based on proton to photon plan comparisons. To improve efficient decision making, we developed a dose mimicking and reducing (DMR) algorithm to automatically generate a robust proton plan from a reference photon dose and target and organs at risk (OARs) delineations.

The DMR algorithm was evaluated in 40 head and neck cancer patients. The first step of the DMR algorithm comprises DVH-based mimicking of the photon dose distribution in the clinical target volumes and OARs. Target robustness is included by mimicking the nominal photon dose distribution in 21 perturbed scenarios. The second step of the optimization aims to reduce the OAR doses while retaining the robust target coverage as achieved in the first step. We evaluated each DMR plan against the 'manually' robustly optimized reference proton plan in terms of plan robustness (voxel-wise minimum dose). Furthermore, the DMR plans were evaluated against the reference photon plan using normal tissue complication probability (NTCP) models of xerostomia, dysphagia and tube feeding dependence. Consequently, ΔNTCPs were defined as the difference between the NTCPs of the photon and proton plans.

The dose distributions of the DMR and reference proton plans were very similar in terms of target robustness and OAR dose values. Regardless of proton planning technique (i.e. DMR or reference proton plan), the same treatment modality was selected in 80% (32/40) of cases based on the ∑ΔNTCPs. In 15% (6/40) of cases a conflicting decision was made based on relatively small dose differences to the OARs (<2.0 Gy).

The DMR algorithm automatically optimizes robust proton plans from a photon reference dose comparable to dosimetrist-optimized proton plans in head and neck cancer patients. This algorithm has been successfully embedded into a framework to automatically select patients for proton therapy based on normal tissue complication probabilities.

5.1 Introduction

Head and neck cancer (HNC) patients are often treated with radiotherapy with or without systemic treatment and/or surgery. Modern radiotherapy includes intensity modulated techniques using either photons or protons. The current standard radiation technique is intensity modulated radiotherapy (IMRT) or volumetric modulated arc therapy (VMAT) aiming at highly conformal target coverage with sparing of non-target tissues. The physical properties of the proton beam (i.e., the Bragg peak) may even further improve dose conformity with less dose to organs at risk (OARs) [1,2]. In particular, the relatively recent introduction of pencil beam scanning (PBS) technology, together with robust multi-field optimization (MFO), has shown the greatest promise in reducing non-target dose, especially in complex target regions such as HNC [3]. Due in part to these benefits, there has been a steep increase in the availability of PBS world-wide, through both new facilities as well as existing facilities upgrading to PBS from older technologies. Despite this however, the capacity for treating HNC cancer patients with proton therapy remains limited.

In the Netherlands, patient selection for proton therapy in HNC is performed using the 'model-based approach', a national framework, which outlines the criteria in which a significant clinical benefit can be expected relative to photon treatments [4,5]. This approach uses normal tissue complication probability (NTCP) models to compare the expected radiation-induced side effects (such as grade 2 xerostomia, dysphagia and grade 3 tube feeding dependence) arising from both proton and photon therapy, based upon the dose distribution of the patient's treatment plan and clinically relevant prognostic factors. If the difference between NTCP values (ΔNTCP) of the two plans is above a pre-defined threshold, the patient is eligible for proton therapy.

Cheng *et al.* developed a pipeline to automatically calculate the preferred treatment modality per patient based on dose, toxicity (i.e. NTCP models) and cost-effectiveness within minutes [6]. The time and resource intensive generation of photon and proton treatment plans for each patient were however not included in their analysis. This is a substantial departmental burden, which would greatly benefit from automation.

Several approaches to (semi-) automated treatment planning have been presented in literature [7-13]. Examples of automated planning tools include the use of knowledge-based planning using previously approved treatment plans of different patients [7,8] and multicriteria optimization methods [9–13]. Recently, McIntosh *et al.* created an automated plan by mimicking a predicted dose distribution directly derived from the planning image and a set of automatically selected previously treated similar patients [14]. They mimicked

photon dose distributions of HNC patients on a voxel-level and demonstrated similar plan quality as compared to dosimetrist-optimized plans. Fredriksson introduced a mimicking algorithm to automatically improve treatment plans by optimization under reference dose constraints [15]. This algorithm uses a reference dose distribution as a starting point and then optimizes further, either on a dose volume histogram (DVH) basis or on a voxel basis to improve a plan without deteriorating the reference dose distribution. All these publications however have only addressed non-robust plan automation for photons.

In this study, we extended the work of Fredriksson [15] towards photon to robust proton dose mimicking and reducing OAR dose optimization. The presented dose mimicking and dose reduction (DMR) algorithm automatically generates a robust MFO proton plan given a reference photon dose distribution and target and OAR delineations, and was evaluated in 40 HNC patients. The first step of the optimization process consists of robust DVH-based mimicking of the target, accounting for range and setup uncertainties. Due to the characteristics of proton beams, there is room to further improve the dose to the non-target tissues. The second step of the optimization therefore aims to reduce the OAR dose as much as possible. The presented reducing OAR dose optimization aims to not deteriorate on target coverage as achieved during the first step, also accounting for plan robustness. The goal of this study was to determine whether this new DMR algorithm was able to generate a robustly optimized proton plan of equal or better 'quality' than the reference, dosimetrist-optimized proton plan. If so, the algorithm could be used within an automated workflow to determine the selection of HNC patients that would benefit from proton therapy the most.

5.2 Material and methods

5.2.1 Patients

Forty HNC patients that were prospectively registered at our institute between September 2014 and June 2016 and that were treated to the primary tumors and to the elective lymph nodal areas, at both sides of the neck, and that had weekly acquired repeat CT images available (as part of our quality assurance programme) were enrolled in this study. All patients were treated with curative intent using IMRT (n = 14) or VMAT (n = 26) with or without concomitant chemotherapy or cetuximab. Tumors were staged with TNM classifications of T1-4, N0-3, and M0-1 and originated in the nasopharynx (n = 4), glottic larynx (n = 6), hypopharynx (n = 5), oropharynx (tonsil: n = 7; base of tongue: n = 6 posterior wall: n = 1), supraglottic larynx (n = 7), oral cavity (n = 2), and other regions (n = 2).

All patients were treated with a simultaneous integrated boost technique comprising the following dose level prescriptions: 70 Gy (in 2 Gy per fraction, 5 fractions per week) to the primary clinical target volume (CTV1) and 54.25 Gy (1.55 Gy per fraction) to the prophylactic lymph node region (CTV2).

5.2.2 Treatment planning

Reference photon plan (Xref)

Dosimetrists optimized all photon plans in the clinical version of the RayStation treatment planning system (v4.5, RaySearch Laboratories AB, Stockholm, Sweden). Each plan was created to adequately cover the planning target volume (PTV) (V95≥98% for PTV1 and PTV2; relative volume receiving 95% of the prescribed dose) with maximum acceptable doses to the spinal cord and brain of 54 and 60 Gy, respectively. The dose distribution to both parotid glands and swallowing structures (including the superior pharyngeal constrictor muscle and supraglottic larynx, according to Christianen *et al.* [16]) was prioritized optimized as described previously [17]. The IMRT plans consisted of 7 equispaced beams (6 MV) with a maximum of 84 segments. The VMAT plans comprised a dual-arc (360˚) with a maximum constrained leaf motion of 0.25 cm/deg. The dose grid was 0.3 x 0.3 x 0.3 cm^3 for all plans. The final photon dose distribution was calculated using a collapsed cone dose engine.

Reference proton plan (Pref)

One dosimetrist created a robustly optimized PBS proton plan using MFO as implemented in RayStation (v4.99.0) for each patient. Four beams were used, including two anterior oblique beams (gantry and couch angles: beam 1 approx. 50˚ and 340˚; beam 2 approx. 310˚ and 20˚) and two beams from posterior oblique direction (gantry and couch angles: beam 3 approx. 150˚ and 0˚; beam 4 approx. 200˚ and 0˚). To minimize any range uncertainties in the shoulder and neck region, only the anterior beams contributed to the caudal part of the target. Moreover, the beam directions were manually chosen such that dose to the parotids was avoided as much as possible. All beams used a 4.0 cm range shifter to allow for adequate coverage of superficial target volumes. The air gap between the range shifter and the patient was kept at minimum.

The PBS plans were created using minimax robust optimization with a range uncertainty of ±3.0 % and an isotropic setup uncertainty of 5.0 mm, equal to the CTV-PTV margin used in the clinical photon plan. The nominal energy available ranged from 70 - 225 MeV. The minimum spot weight was 0.01 monitor units per spot. The spot and layer spacing was set to 'automated scale 1.0'. The Pref plans were prioritized optimized using robust minimum dose objectives for the CTVs, a dose fall-off objective for the body contour, and dose fall-off objectives as well as maximum equivalent uniform dose objectives (with dose-volume effect parameter α = 1) for the OARs.

5.2.3 Pipeline model-based approach

The model-based approach has previously been introduced to select the preferred treatment modality for the individual patient, based on NTCP model prediction [4]. The selection is based on ΔNTCP values as derived from e.g. a photon and a proton dose distribution and evaluated against predefined thresholds. If the pre-established ΔNTCP threshold is exceeded, the patient is referred for proton therapy, otherwise the patient receives photon radiotherapy. Figure 5.1 illustrates how ΔNTCP is derived using the DMR algorithm given a reference photon dose distribution and corresponding decision criteria. The NTCP models as well as the thresholds for different grades of complication are shown in table 5.1. These NTCP models and thresholds have recently been established in the 'Dutch National Indication Protocol for Proton Therapy' [18].

Figure 5.1. *Flow chart of the dose mimicking and reducing (DMR) algorithm embedded in the pipeline for ΔNTCP assessment.*

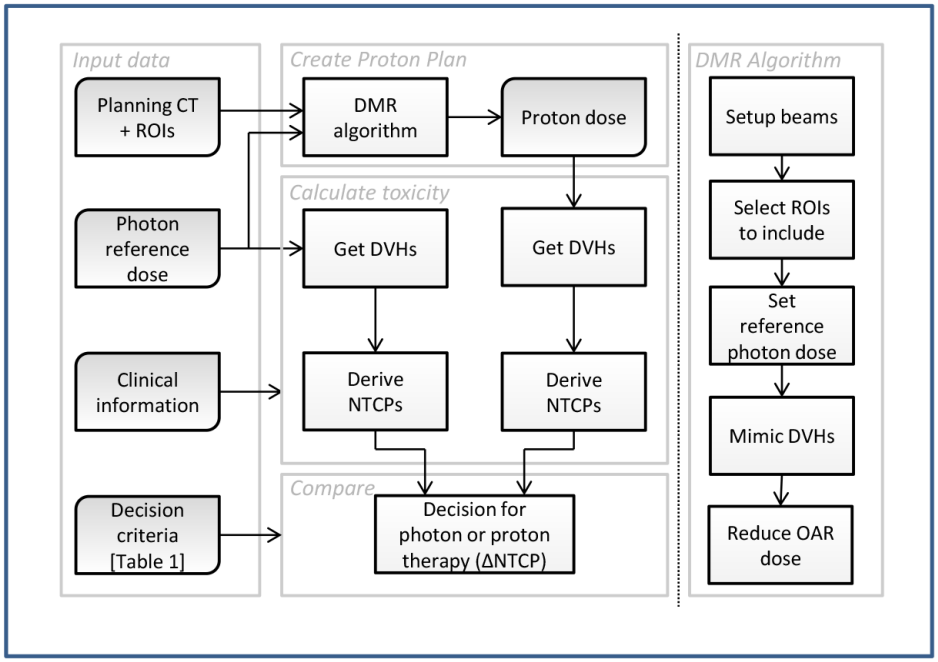

Clinical information denotes the non-DVH predictors. The right panel shows the DMR algorithm in more detail as applied to proton automated treatment planning. DVH denotes dose volume histogram, ROI region of interest, and NTCP normal tissue complication probability.

Table 5.1. *NTCP models and decision criteria*

NTCP model	*Organ(s) involved (all mean dose)*
Xerostomia (6 mo; grade 2-3)	Contralateral parotid
Dysphagia (6 mo; grade 2-3)	Oral cavity; superior PCM
Tube feeding dependence (6 mo; grade 3-4)	Contralateral parotid; superior PCM; inferior PCM; cricopharyngeal muscle.
Decision criteria	ΔNTCP
ΔNTCP of any grade ≤ 2 complication	≥ 10%
ΔNTCP of grade 3+ complication	≥ 5%
∑ΔNTCP of grade ≤ 2 complication	≥ 15 %

Abbreviation: PCM = pharyngeal constrictor muscle.

5.2.4 Dose mimicking

PBS proton treatment plans were automatically generated using an extended version of the original 'reducing OAR dose' algorithm as described by [15]. Our extension comprised of photon to robust proton dose mimicking and was implemented in a research version of RayStation (v5.99.0). The DMR algorithm consists of the following components, as illustrated in figure 5.1:

- The beam angles are selected.
- The ROIs that are to be considered in the optimization are selected.
- The reference dose is set to the dose distribution of the photon plan to be mimicked.
- A robust dose mimicking optimization is performed using 21 perturbed scenarios.
- A robust 'reducing OAR dose optimization' is performed using 21 perturbed scenarios.

In the present study, the algorithm was instantiated as follows:
To avoid any bias from proton beam angle selection, the beam configuration (step 1) of the DMR plans was copied from the reference proton plans. In the ROI selection (step 2), the CTVs and OARs related to patient-rated xerostomia, grade 2-4 dysphagia and tube feeding dependence, and the spinal cord were included (see table 5.1). Then the reference dose distribution is set to Xref (step 3).

In the mimicking part (step 4), the DMR algorithm comprised DVH-based mimicking of Xref in the CTVs and OARs. This optimization aims to achieve a proton plan that has at least similar target coverage, also when uncertainty is considered, and at least similar OAR sparing as in the photon dose set in step 3. The DVH-based mimicking minimized the deviation between the DVHs of Xref and those of the proton plan being optimized. Plan robustness was only considered for the targets, and achieved by mimicking the nominal photon dose distribution in each uncertainty scenario. Mathematically, the DVH-based mimicking utilizes the function $D_r^{\text{ref}}(v)$, which parameterizes the DVH of ROI *r* in the photon reference dose distribution as a function of the fraction $v \in [0,1]$ of the ROI volume, i.e.,

$D_r^{\text{ref}}(0.9)$ is D90 in the photon reference dose distribution. It also utilizes the function $D_r(v; x, s)$, which is like $D_r^{\text{ref}}(v)$, but in the dose distribution of the proton plan being optimized for the spot weights *x* under scenario *s*. The objective function, which is to be minimized, is formulated as

$$\sum_{r \in O} \int_0^1 \max(D_r(v; x, s_0) - D_r^{\text{ref}}(v), 0)\, dv \; + \sum_{s \in S} \sum_{r \in T} \int_0^{v_r} \max(D_r(v; x, s) - D_r^{\text{ref}}(v), 0)\, dv$$
$$+ \sum_{s \in S} \sum_{r \in T} \int_{v_r}^1 \max(D_r^{\text{ref}}(v) - D_r(v; x, s), 0)\, dv \;,$$

where *O* is the set of considered OARs, *T* is the set of considered targets, *S* is the set of considered scenarios, and S_0 denotes the nominal (planning) scenario. The parameter v_r specifies where over- and underdosage should be penalized for targets. Per default, it was set to 0.5, but to include the dose gradient between low and high dose targets more accurately, it was set to 0.9 for targets where (D10 - D90) / D10 > 0.2 in Xref, which was the case for CTV2 in the studied patients. To illustrate, when the dose of the fractional volume *v* lies within the grey area (as in figure 5.3, bounded by the reference photon DVH), the dose is penalized by the objective function (third part of abovementioned formula).

In the 'reducing OAR dose optimization' step (step 5), the DMR algorithm aimed to reduce OAR doses as much as possible while retaining the plan quality achieved in step 4 in a DVH-based fashion. To this end, constraints were introduced preventing the DVHs of the plan to deteriorate compared to the proton mimicking plan of step 4. Under each uncertainty scenario, the DVH of each target was constrained not to deteriorate compared to the DVH of the mimicking plan in the same scenario. Fredriksson describes this fifth step of the DMR algorithm, without considering robustness [15]. Mathematically, the OAR dose reduction optimization problem uses the functions from the DVH-based mimicking objective as constraints, but substitutes the function $\boldsymbol{D_r^{\text{ref}}(v; s)}$ for $D_r^{\text{ref}}(v)$, where $\boldsymbol{D_r^{\text{ref}}(v; s)}$ parameterizes the DVH of ROI *r* in the dose distribution under scenario *s* of the proton plan achieved by the mimicking in step 4. The objective function, which is to be minimized, is formulated as

$$\sum_{r \in O} \int_0^1 D_r(v; x, s_0)\, dv,$$

and the constraints as

$$\sum_{r \in O} \int_0^1 \max(D_r(v; x, s_0) - D_r^{\text{ref}}(v; s_0), 0)\, dv \;\; \leq 0,$$

$$\sum_{s \in S} \sum_{r \in T} \int_0^{v_r} \max(D_r(v; x, s) - D_r^{\text{ref}}(v; s), 0)\, dv \;\; \leq 0,$$

$$\sum_{s \in S} \sum_{r \in T} \int_{v_r}^1 \max(D_r^{\text{ref}}(v; s) - D_r(v; x, s), 0)\, dv \;\; \leq 0.$$

The DMR optimization time (step 2 – 5) depended on the number of iterations, the number of dose grid voxels and target size and ranged from approximately 120 to 240 minutes in RayStation v5.99[1]. The dose mimicking optimization (step 4) contained three optimizations rounds each with 50 iterations. The reducing OAR dose optimization (step 5) was performed with 50 iterations.

5.2.4 Analysis

For each proton plan (i.e. DMR and Pref plan), plan robustness was assessed by evaluating the treatment plan under 14 rigidly perturbed and equally distributed setup error scenarios. The collection of scenarios is sampled from a cube and projected on a sphere with radius M. In total, 8 vertices (x=±M/√3, y=±M/√3, z=±M/√3) and 6 faces (±M, 0,0); (0, ±M, 0); (0, 0, ±M) were used to derive the scenarios. For all scenarios the image was scaled by ±3% to account for range uncertainty. From the resulting 28 scenarios, a voxel-wise minimum dose distribution was constructed from which the V95% of the CTV was derived and compared between the DMR and Pref plan. In addition, plans were evaluated in terms of (Δ)NTCP values (see table 5.1) and target conformity ($CI_{V95\%}$). The $CI_{V95\%}$ was defined as the ratio between the absolute volume of the 95% isodose line and the V95% in the CTV.

5.3 Results

The DMR algorithm created clinically realistic robust treatment plans that were comparable to the reference proton plans in terms of target robustness and OAR dose. The photon dose distribution (i.e. Xref) and the voxel-wise minimum dose of the DMR and Pref of a representative case are shown in figure 5.2. The target coverage of the nominal scenario was very similar in the photon and proton plans (see target DVHs in figure 5.3). The DVHs indicated the result of the 'dose mimicking' step as well as the 'reducing' step. The latter indicates a clear reduction of OAR dose whereas the targets remained constrained to the target DVH of the reference photon plan.

1 Within RayStation v6.99, the optimization times improved substantially ranging from approximately 60 –120 minutes.

In 80% (32/40) of the cases, the DMR algorithm selected the same patients for proton therapy as if Pref was used for patient selection. In 15% (6/40) of cases a conflicting decision was made based on relatively small (approx. <2.0 Gy) dose differences to the OARs. For these borderline cases, one plan (e.g. the DMR plan) would meet the decision criteria for proton therapy selection in terms of ∑ΔNTCP thresholds, whereas the other plan (e.g. Pref plan) would not qualify for proton therapy (or vice versa). In 5% (2/40) of the

cases the target DVH of Xref was already compromised. Consequently, the target DVH of the DMR plan was compromised resulting in too optimistic OAR doses (and NTCP values) and conflicting decisions compared to the reference proton plan.

Figure 5.2. *A transversal cross-section of a CT scan of a representative case with the nominal dose distribution of the clinical photon plan (left), the voxel-wise minimum dose of the robust dose mimicking and reducing (DMR) proton plan (middle), and the voxel-wise minimum dose of the dosimetrist-optimized reference robust proton plan (right).*

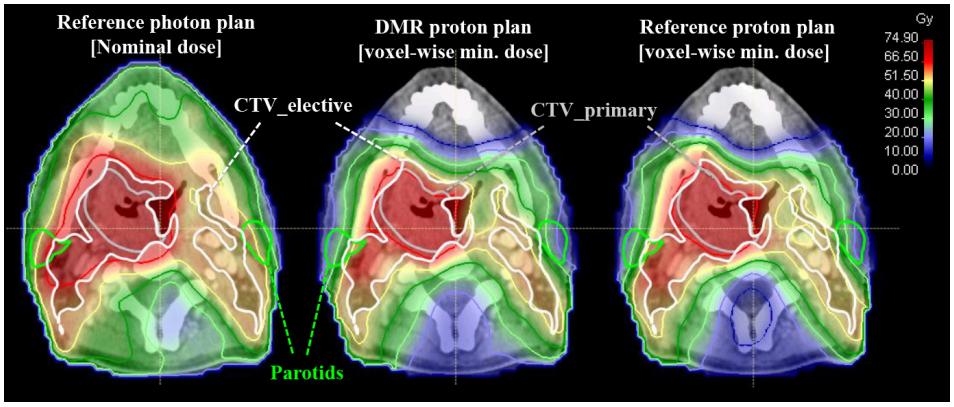

With the DMR plans 10% more patients of the studied cohort qualified for proton therapy as compared to the Pref plans. The differences between the ∑ΔNTCP values derived from the DMR and the Pref plans were however small: on average (±1.96 SD) 2.2 (±12.3) % (figure 5.4a). The scatter plot (figure 5.4b) shows high agreement between the NTCP values of xerostomia, grade 2-4 dysphagia, and tube feeding dependence as derived from the DMR and Pref plan.

The difference of V95% of the voxel-wise minimum dose between the DMR and the Pref plan was <0.05 in 35/40 and 37/40 of the cases for CTV1 and CTV2, respectively (figure 5.5a). The two outliers indicate the DMR plans that were optimized given an underdosed target DVH of the reference photon plans. The $CI_{V95\%}$ of the voxel-wise minimum dose indicated that the DMR and Pref plan had, on average, similar target dose conformity for CTV1 (t-test using the 0.05 significance level: $p = 0.16$).

Figure 5.3. *Dose-volume histograms of the high (red) and low (green) dose clinical target volumes and the medial pharyngeal constrictor muscle (blue) and the contralateral parotid gland (orange).*

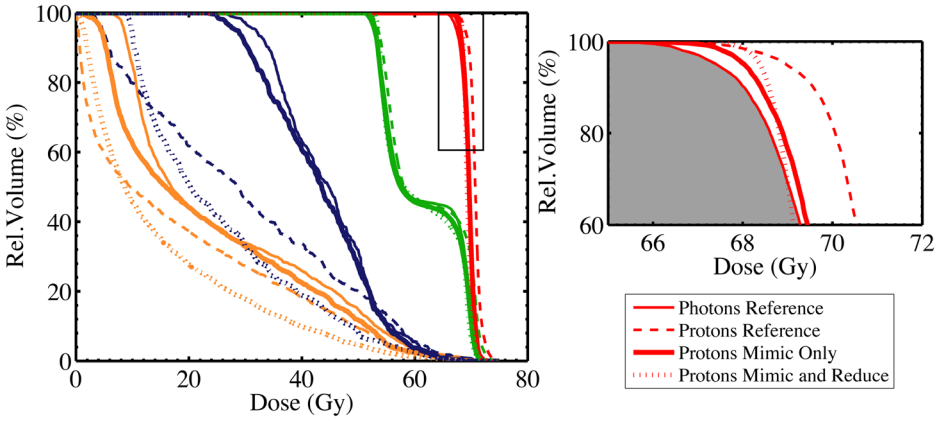

The legend indicates the plan type. The inlay shows the high dose target DVHs in more detail. The DVH-based mimicking of the target DVH is penalized within the grey surface, bounded by the photon reference DVH.

On average (±1.96 SD), the $CI_{V95\%}$ of the voxel-wise minimum dose distribution of CTV2 was 0.22 (±0.41) ($p < 0.001$) lower for the Pref plan than for the DMR plan, indicating slightly more conformal target coverage of the voxel-wise minimum dose distribution of the Pref plans (figure 5.5b).

Figure 5.4. *(A) Bland-Altman plot of the difference of the ∑ΔNTCP derived from the dose mimicking and reducing (DMR) plan and reference proton plan Pref.*

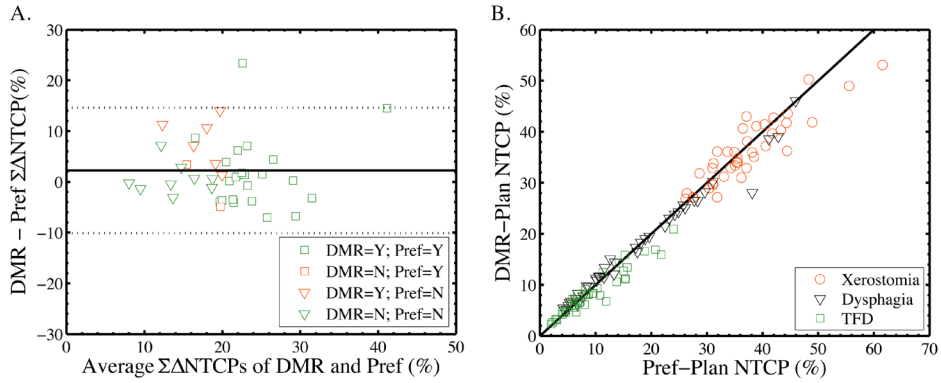

The green markers indicate agreement between the selected treatment modality (Y = protons; N = photons). The orange markers indicate conflicting decisions. (B) Normal tissue complication probability (NTCP) values of xerostomia, grade 2-4 dysphagia, and tube feeding dependence (TFD) derived from the DMR plans and Pref plans.

Figure 5.5. *Bland-Altman plots of the relative volume receiving 95% of the prescribed dose (A) and the conformity index $CI_{V95\%}$ (B) as derived from the voxel-wise minimum dose of the dose mimicking and reducing (DMR) plan and reference proton plan Pref.*

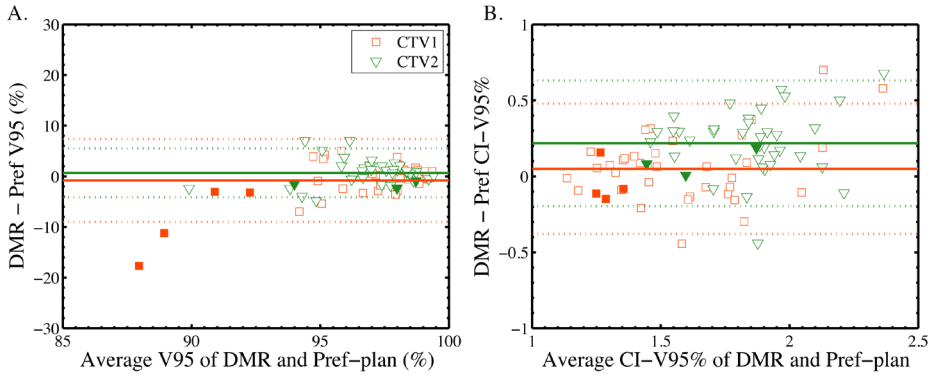

CTV1 and CTV2 denotes the clinical target volume of the high and low dose targets, respectively. The solid markers indicate the plans with compromised target coverage of the reference photon plan.

5.4 Discussion

The dose 'mimicking and reducing' algorithm turned a photon dose distribution into a robust MFO proton plan comparable to the dosimetrist-optimized proton plan for 40 HNC patients. We simulated the model-based approach within this cohort (i.e. the calculation of ∑ΔNTCP values from the proton and photon dose distribution) and found that the DMR algorithm selected 80% of cases for the same treatment technique as when the reference proton plan was used. The DMR algorithm therefore can play a big role in automated planning and could also be used within the model-based approach pipeline to select patients for proton therapy.

Dose mimicking has been presented previously and focussed on photon dose distributions only [14,15]. A voxel and DVH-based mimicking algorithm was introduced by Fredriksson to automatically improve a given reference photon dose [15]. The author evaluated the algorithm in a phantom study and found that the dose of the reference plan could further reduce the OARs dose while maintaining target coverage. McIntosh *et al.* applied a dose mimicking algorithm to a predicted dose distributions derived from dose distributions of a set of similar patients to automatically create a photon treatment plan for novel patients [14]. In this study we extended the dose mimicking algorithm from Fredriksson [15] toward photon to robust proton based dose mimicking. Also, the reducing OAR dose optimization part was extended to account for target robustness, taking multiple error scenarios into account.

We acknowledge that the automated planning algorithm did not include automated beam angle selection. Therefore, we copied the beam configurations from the reference proton plan and automated beam angle selection will be subject of ongoing research. Moreover, to avoid inter-planner variability, all reference proton plans were created by one dosimetrist (M. Gelderman). The reference photon plans were however extracted from the clinical database and generated by a variety of dosimetrists. This directly corresponds to the current clinical workflow for patient selection for proton therapy.

Improving the target coverage has not been investigated in this study. It can sometimes be the case that photon plans have inadequate target coverage, especially if the target is close to the patient surface (due to the photon build-up effect), or due to proximity of dose-limiting critical structures (e.g. the optic structures). With a photon reference dose distribution, the DMR algorithm currently does not seek to improve on it even though it may be possible with PBS and since the DMR algorithm in this study used DVH-mimicking, any target underdosage in the photon plan will carry through into the proton plan, although not necessarily in the same region. In these (few) cases, the dosimetrist-optimised proton plan had the more clinically acceptable dose distributions. It is therefore important that the reference photon plans have sufficient target coverage to begin with. If target coverage of the photon plans was compromised, one could utilize all slack that is gained from selecting protons to improve OARs (as has been done in this study), or utilize some to also improve target coverage. Therefore, and also to study the full potential of the DMR algorithm, the DMR algorithm should be combined with e.g. a clinical goal-based normalization method for photon plans with underdosage. This was however outside the scope of the present study.

Future research will focus on the application of dose mimicking for adaptive treatments. The goal is to achieve at least the same target DVHs of the original plan onto the repeat CT. Moreover, to further improve the photon dose, the 'reducing' function can be applied onto the photon dose distribution before patient treatment selection is performed. This would potentially reduce the NTCP values derived from the photon plan and consequently lead to a fairer selection of patients for proton therapy.

In conclusion, the DMR algorithm automatically optimized a robust proton plan using a photon reference dose distribution. We developed a fully automated tool to select head and neck cancer patients for proton therapy by combining the DMR algorithm with the model-based approach.

5.5 References

[1] Brada M, Pijls-Johannesma M, Ruysscher D De. Current clinical evidence for proton therapy. Cancer J 2009;15:319–24. doi:10.1097/PPO.0b013e3181b6127c.

[2] van de Water T A, Lomax AJ, Bijl HP, de Jong ME, Schilstra C, Hug EB, *et al*. Potential benefits of scanned intensity-modulated proton therapy versus advanced photon therapy with regard to sparing of the salivary glands in oropharyngeal cancer. Int J Radiat Oncol Biol Phys 2011;79:1216–24. doi:10.1016/j.ijrobp.2010.05.012.

[3] Lomax AJ, Böhringer T, Bolsi A, Coray D, Emert F, Goitein G, *et al*. Treatment planning and verification of proton therapy using spot scanning: Initial experiences. Med Phys 2004;31:3150–7. doi:10.1118/1.1779371.

[4] Langendijk J A, Lambin P, De Ruysscher D, Widder J, Bos M, Verheij M. Selection of patients for radiotherapy with protons aiming at reduction of side effects: the model-based approach. Radiother Oncol 2013;107:267–73. doi:10.1016/j.radonc.2013.05.007.

[5] Widder J, van der Schaaf A, Lambin P, Marijnen CAM, Pignol J-P, Rasch CR, *et al*. The Quest for Evidence for Proton Therapy: Model-Based Approach and Precision Medicine. Int J Radiat Oncol Biol Phys 2016;95:30–6.

[6] Cheng Q, Roelofs E, Ramaekers BLT, Eekers D, Van Soest J, Lustberg T, *et al*. Development and evaluation of an online three-level proton vs photon decision support prototype for head and neck cancer - Comparison of dose, toxicity and cost-effectiveness. Radiother Oncol 2016;118:281–5. doi:10.1016/j.radonc.2015.12.029.

[7] Chanyavanich V, Das SK, Lee WR, Lo JY. Knowledge-based IMRT treatment planning for prostate cancer. Med Phys 2011;38:2515–22. doi:10.1118/1.3574874.

[8] Appenzoller LM, Michalski JM, Thorstad WL, Mutic S, Moore KL. Predicting dose-volume histograms for organs-at-risk in IMRT planning. Med Phys 2012;39:7446–61. doi:10.1118/1.4761864.

[9] Craft DL, Halabi TF, Shih H A., Bortfeld TR. Approximating convex Pareto surfaces in multiobjective radiotherapy planning. Med Phys 2006;33:3399. doi:10.1118/1.2335486.

[10] Breedveld S, Storchi PRM, Keijzer M, Heemink AW, Heijmen BJM. A novel approach to multi-criteria inverse planning for IMRT. Phys Med Biol 2007;52:6339–53. doi:10.1088/0031-9155/52/20/016.

[11] Thieke C, Küfer K-H, Monz M, Scherrer A, Alonso F, Oelfke U, *et al*. A new concept for interactive radiotherapy planning with multicriteria optimization: first clinical evaluation. Radiother Oncol 2007;85:292–8. doi:10.1016/j.radonc.2007.06.020.

[12] Bokrantz R. Multicriteria optimization for volumetric-modulated arc therapy by decomposition into a fluence-based relaxation and a segment weight-based restriction. Med Phys 2012;39:6712–25. doi:10.1118/1.4754652.

[13] Fredriksson A, Bokrantz R. Deliverable navigation for multicriteria IMRT treatment planning by combining shared and individual apertures. Phys Med Biol 2013;58:7683–97. doi:10.1088/0031-9155/58/21/7683.

[14] McIntosh C, Welch M, McNiven A, Jaffray DA, Purdie TG. Fully Automated Treatment Planning for Head and Neck Radiotherapy using a Voxel-Based Dose Prediction and Dose Mimicking Method 2016. doi:10.1088/1361-6560/aa71f8.

[15] Fredriksson A. Automated improvement of radiation therapy treatment plans by optimization under reference dose constraints. Phys Med Biol 2012;57:7799–811. doi:10.1088/0031-9155/57/23/7799.

[16] Christianen MEMC, Schilstra C, Beetz I, Muijs CT, Chouvalova O, Burlage FR, *et al*. Predictive modelling for swallowing dysfunction after primary (chemo)radiation: results of a prospective observational study. Radiother Oncol 2012;105:107–14. doi:10.1016/j.radonc.2011.08.009.

[17] van der Laan HP, Christianen M, Bijl HP. The potential benefit of swallowing sparing intensity modulated radiotherapy to reduce swallowing dysfunction: an in silico planning comparative study. Radiother Oncol 2012;103:76–81. doi:10.1016/j.radonc.2011.11.001.